Annual variations in sea surface height northeast of the Hawaiian Islands

Shuiming Chen[1] and Bo Qiu[1]

Received 23 May 2006; revised 18 July 2006; accepted 26 July 2006; published 15 September 2006.

[1] A decade-long satellite altimeter data set is used to analyze the annual variations in the sea surface height (SSH) field northeast of the Hawaiian Islands. The annual harmonic amplitudes for the SSH and the along-island geostrophic flow are 2–4 cm and 2–4 cm s^{-1}, respectively. Although these values are an order of magnitude smaller than the regional mesoscale eddy signals, the annual SSH signals have a robust spatial structure that can be expressed as a function of distance northeastward away from the Hawaiian Islands. The annual SSH signals are then described by using trapped annual waves and a basin-scale non-propagating signal. Using the linearized vorticity equation, we suggest that the trapped annual waves are baroclinic Rossby waves that decay from the Hawaiian Islands. **Citation:** Chen, S., and B. Qiu (2006), Annual variations in sea surface height northeast of the Hawaiian Islands, *Geophys. Res. Lett.*, *33*, L17612, doi:10.1029/2006GL027005.

1. Introduction

[2] Mesoscale eddy variability on timescales of 3–6 months has been shown to be high in the region northeast of the Hawaiian Islands [e.g., *Van Woert and Price*, 1993; *Mitchum*, 1996; *Chiswell*, 1996; *Polito et al.*, 2000]. At Station ALOHA (158°W, 22.75°N), about 100 km northeast of the Hawaiian Islands, surface dynamic height signals varied by as much as 27 dynamical cm on timescales of about 100 days [*Chiswell*, 1996]. It is also known that except for within the surface mixed layer, the annual cycles of physical properties in this region are relatively weak but some of them can be significant. For example, annual variations of salinity and oxygen at intermediate waters, accounting for as much as 25% of the total variance, were observed at Station ALOHA [*Bingham and Lukas*, 1996].

[3] With the advent of satellite altimetry, several studies in the past have focused on the annual cycle of the sea surface height (SSH) field. The annual harmonics of SSH have been derived for the North Pacific Ocean by *Jacobs et al.* [1993] using GEOSAT data, and for the global ocean by *Stammer* [1997] using the first three years of Topex/Poseidon (T/P) data. The analyses by *Vivier et al.* [1999] and *Polito et al.* [2000] have further decomposed the annual SSH signals into those associated with the steric height, baroclinic Rossby waves, time-varying topographic Sverdrup balance, and Ekman pumping response. While most of the above-mentioned studies have focused on basin-scale features, some did mention regional phenomena. Of particular interest to this study is Figure 9 of *Jacobs et al.* [1993], showing the wave crests of the annual SSH harmonics being parallel to the Hawaiian Islands. *Jacobs et al.* [1993] suspected that those wave crests are barotropic Rossby waves generated at the equator. The purpose of the present study is first, to describe the annual SSH variations in the region northeast of the Hawaiian Islands using the now-available, decade-long altimetry data and second, to explore the mechanism underlying the observed annual variations.

2. Altimetry Observation

[4] Our principle data set is the merged AVISO SSH anomaly product. By using the method presented by *Stammer* [1997], an annual steric height signal, which is forced by the 1992–2004 NCEP surface heat flux and is basin-scale without any visible variations across the Hawaiian Islands, is subtracted before the harmonic analysis is performed.

[5] In Figure 1, the high-pass filtered (two-year cutoff) SSH time series northeast of the Hawaiian Islands reveals that the annual SSH signal is discernible in all years except 1993–1994 and 2000–2001. Despite the strong mesoscale eddy signals, the altimeter measurements indicate that the annual SSH signals are observable in the region northeast of the Hawaiian Islands.

[6] The spatial distribution of the annual amplitudes of the SSH near the Hawaiian Islands is shown in Figure 2a. The amplitudes are small adjacent to the Hawaiian Islands, then increase northeastward, reaching a maximum at about 2–3° latitude northeast of the Hawaiian Islands. Further offshore, the amplitudes decrease and increase alternately. Figure 2b shows the phase of the annual cycle; the value (in deg.) indicates the time when SSH reaches the annual maximum, with zero deg. corresponding to January 1st. East of the Hawaiian Islands the annual phases are mostly

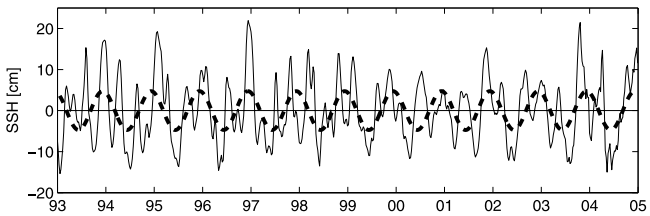

Figure 1. High-pass filtered (two-year cutoff) time series of the AVISO SSH (thin line) and the annual harmonics (thick dashed line) at 164.8°W, 25.9°N. The location is shown by the black dot in Figure 2a.

[1]Department of Oceanography, University of Hawaii at Manoa, Honolulu, Hawaii, USA.

0094-8276/06/2006GL027005$05.00

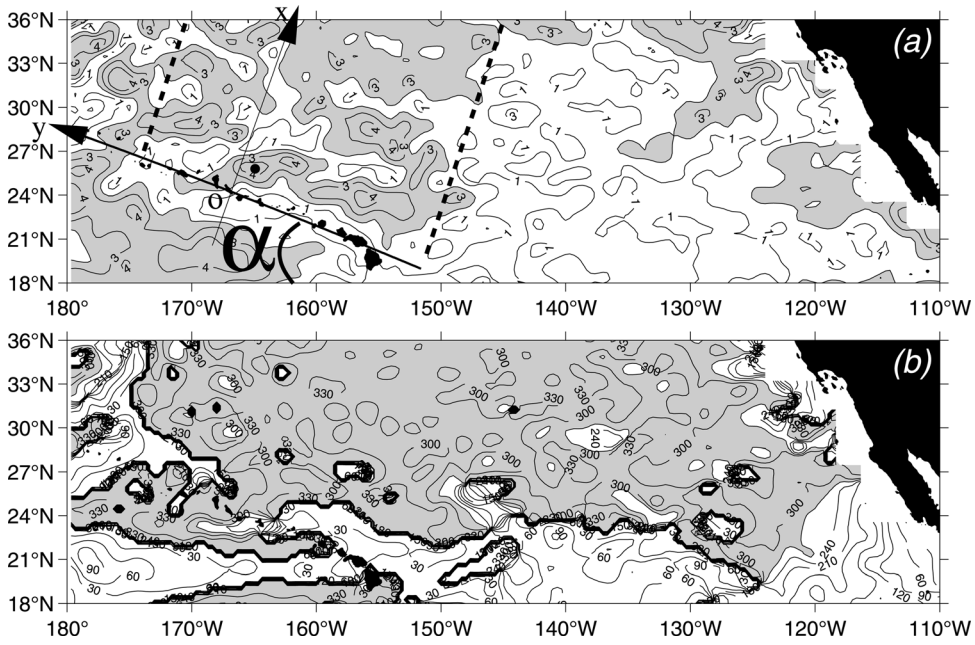

Figure 2. (a) Annual amplitudes of the altimetric SSH, in cm. Areas with amplitudes larger than 2 cm are gray-shaded. Along the Hawaiian Islands, the dark shading shows areas shallower than 500 m. The across- and along-islands Cartesian coordinate *xoy* is indicated. The y-axis ($\alpha = 20^\circ$ from the west), along with the two thick dashed lines and the 36°N line, indicates the domain where the AVISO SSH date are used in Figure 3. The high-pass filtered SSH time series at the black dot northeast of the Hawaiian Islands is shown in Figure 1. (b) Annual phases of the altimetric SSH, in degrees. Areas with phases between 270–360° are gray-shaded. Contours are clustered where the phases jump from 0 to 360°.

in the range of 300 ∼ 330° (i.e. November). This is consistent with the results of *Stammer* [1997, Plate 6f].

[7] Figures 3a and 3b show scatter plots of the amplitudes and phases of the annual SSH signals as a function of distance away from the islands. At each snapshot surface geostrophic velocities between SSH grids are calculated and projected onto the along- and across-islands directions (see Figure 2a for orientation). The annual amplitudes and phases for the along-islands, surface geostrophic flow are shown in Figures 3c and 3d. As found in Figure 2a, Figure 3a shows that the SSH amplitudes are small adjacent to the islands, reach a maximum about 220 km northeast of the islands, and fluctuate with amplitudes of ∼2.25 cm further offshore. The phases of the along-islands geostrophic flow increase monotonically towards the islands (Figure 3d), suggesting that this part of the annual signal consists of propagating waves.

[8] To interpret the observations in Figure 3 (gray crosses), we assume that the annual SSH (h) and the annual along-islands geostrophic velocity (v) can be expressed by

$$h(x,t) = Be^{-k_i x}\cos(k_r x - \omega t + \theta_1) + C\cos(\omega t - \theta_2) \quad (1)$$

$$v(x,t) = \frac{g}{f}\frac{\partial h}{\partial x} = -\frac{Bg}{f}[k_r \sin(k_r x - \omega t + \theta_1) + k_i \cos(k_r x - \omega t + \theta_1)]e^{-k_i x}, \quad (2)$$

where x is the distance away from the Hawaiian Islands (see Figure 2a), t time, ω the annual frequency, g gravitational acceleration, and f the Coriolis parameter at 24°N. We will refer to the first part of the r.h.s. of equation (1) as the trapped annual wave (decay away from the islands in the form of $e^{-k_i x}$) and the second part as the basin-scale non-propagating annual signal, with amplitudes B and C, respectively. Equation (1) implicitly assumes that the annual signals do not vary in the along-islands direction, an assumption supported by the across-islands banding of the SSH annual amplitudes (Figures 2a and 3a) and by the tightness of the along-islands geostrophic flow phases (Figure 3d). From equation (1), the annual amplitudes and phases of the SSH and of the along-islands geostrophic flow ($A_h(x)$, $\alpha_h(x)$, $A_v(x)$, $\alpha_v(x)$) can be expressed as functions of x, with B, C, k_r, k_i, θ_1, and θ_2 being the parameters to be estimated in the least squares sense.

[9] Before fitting $A_h(x)$, $\alpha_h(x)$, $A_v(x)$, and $\alpha_v(x)$ to the data, we grid the altimetric observations in 30-km bins based on distance northeast of the Hawaiian Islands. The gridded observations (bin averages) $A_h^\circ(x_i)$, $\alpha_h^\circ(x_i)$, $A_v^\circ(x_i)$, $\alpha_v^\circ(x_i)$ (i = 1, 2, ⋯, N, and x_1 = 15 km, x_2 = 45 km, ⋯) are presented as dark crosses in Figures 3a–3d, respectively. In each 30-km bin, we also obtain the variances of corresponding quantities; their medians over all N bins are denoted as $var(A_h^\circ)$, $var(\alpha_h^\circ)$, $var(A_v^\circ)$, and $var(\alpha_v^\circ)$, respectively.

[10] To reduce the number of free parameters to be fitted, we chose C = 2.25 cm and θ_2 = 315°, by inspection of Figures 3a and 3b. We use amplitudes of the SSH, phases of the SSH, and phases of the along-islands geostrophic flow

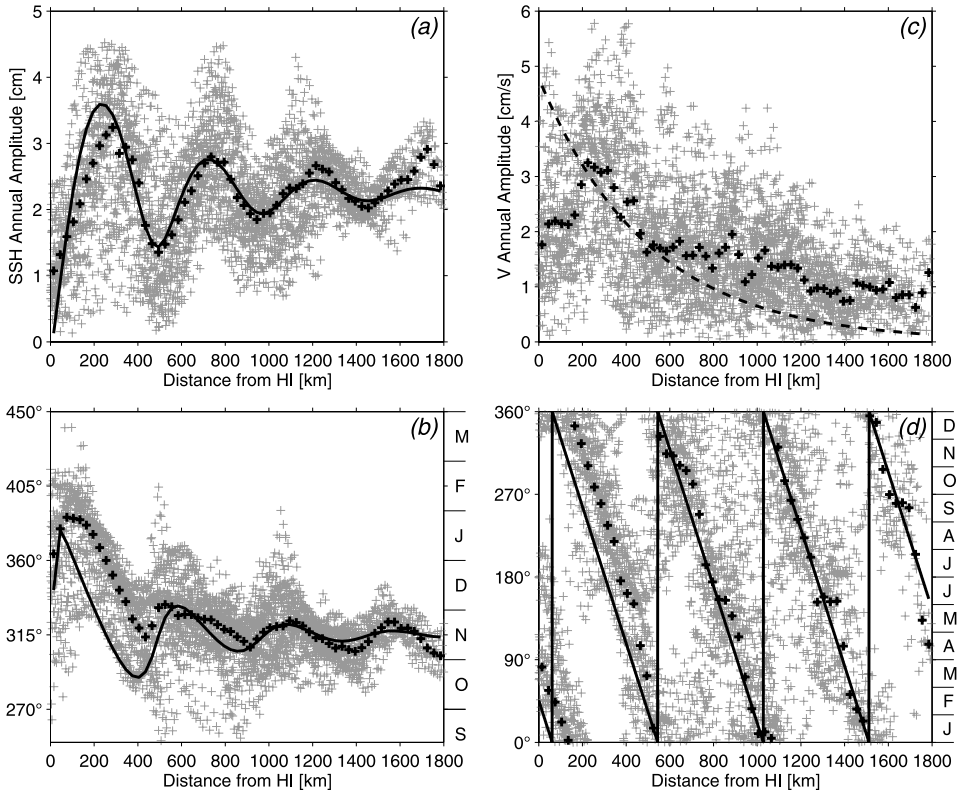

Figure 3. Gray crosses are based on the AVISO 1/3° × 1/3° gridded data in the domain limited by the y-axis, the two thick dashed lines, and the 36°N line shown in Figure 2a. Distance refers to the northeastward distance normal to the Hawaiian Islands, corresponding to the positive x axis in Figure 2a. Dark crosses are the averages over 30-km distance bins, and solid and dashed lines are based on the lease-squares fitting described in the text. (a and b) Annual amplitudes and phases of the altimetric SSH. (c and d) Annual amplitudes and phases of the along-islands geostrophic flow. In Figures 3b and 3d, months are indicated at the right sides.

to seek the parameters (B, k_r, k_i, θ_1) by minimizing the following cost function:

$$J = \frac{\sum_1^N \left[A_h(x_i) - A_h^\circ(x_i)\right]^2}{var\left(A_h^\circ\right)} + \frac{\sum_1^N \left[\alpha_h(x_i) - \alpha_h^\circ(x_i)\right]^2}{var\left(\alpha_h^\circ\right)} + \frac{\sum_1^N \left[\alpha_v(x_i) - \alpha_v^\circ(x_i)\right]^2}{var\left(\alpha_v^\circ\right)}.$$

The results are B=2.2 cm, $1/k_i$ = 500 km, $1/k_r = -77$ km (wavelength $2\pi/|k_r|$ is about 484 km), and θ_1=145°. Since wavenumber $k_r < 0$, the trapped annual waves propagate towards the islands. The resulting $A_h(x_i)$, $\alpha_h(x_i)$, $\alpha_v(x_i)$ are represented in Figures 3a, 3b, and 3d, respectively, by solid lines. The annual amplitude of the along-islands geostrophic flow $A_v(x)$ is then calculated, and it is shown in Figure 3c by the thick dashed line.

[11] Our fitting assumes that the annual signals consist of trapped waves and a basin-scale, non-propagating signal. Under this assumption, the smallness of the SSH annual variation adjacent to the islands is due to these two types of annual signals having similar magnitudes, but being nearly out of phase at the islands (θ_1 = 145° and θ_2 = 315° at x = 0). Similarly, the maximum of the SSH annual amplitude at about 220 km is due to these two

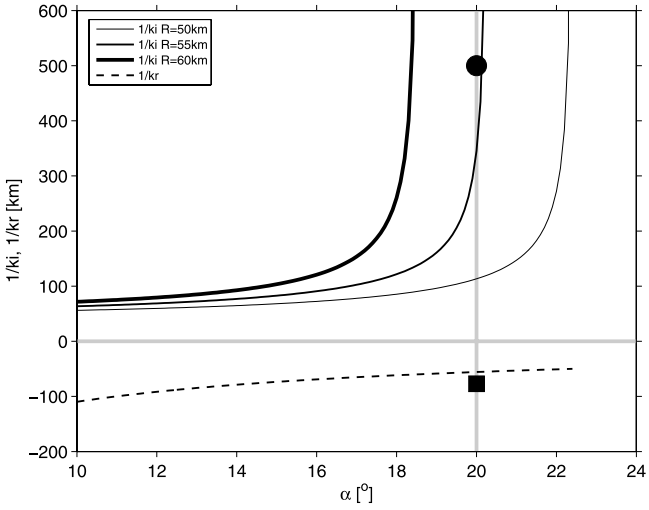

Figure 4. $1/k_r$ and $1/k_i$ (reciprocals of the real and imaginary components of wavenumber k in equation (6)) are plotted as functions of angle α. $1/k_r$ (dashed line) does not depend on R. $1/k_i$ (solid lines) is shown for three values of R (50, 55, and 60 km). The solid circle and solid square represent the $1/k_i$ and $1/k_k$ obtained from fitting the satellite observations, respectively.

annual signals being approximately in phase at that location. Meanwhile, noticeable deficiencies of the fitting are seen adjacent to the islands; they are probably caused by the energetic eddies in the region and by topographic, frictional or other near coastal effects.

3. Discussion

[12] We described the annual signals of the SSH northeast of the Hawaiian Islands in terms of trapped waves and a basin-scale non-propagating annual signal. The first question is whether these signals are simple responses to local forcing.

[13] East of the Hawaiian Islands, the mean curl of the northeast trade-wind stress is as large as 8×10^{-8} Nm^{-3}, but the annual amplitude of the wind stress curl ranges from 1×10^{-8} Nm^{-3} near the North American west coast to 3×10^{-8} Nm^{-3} adjacent to the Hawaiian Islands. The Ekman pumping associated with the annual wind stress curl variations near the islands would directly force an annual SSH oscillation on order of 1 cm. This can be demonstrated by using the Ekman pumping balance in a $1^1/_2$ -layer model: $\frac{\partial h}{\partial t} = -\frac{g'}{g}\nabla \times \frac{\vec{\tau}}{\rho_0 f}$, where h is the SSH and all other variables have their conventional meanings [*Kessler*, 1990]. At 24°N, the annual amplitude of SSH, h, is approximately $\frac{g'}{g}\frac{\nabla\times\vec{\tau}}{\rho_0 f\omega} \approx 0.8$ cm for an annual wind stress curl oscillation with an amplitude of 3×10^{-8} Nm^{-3}, and for $g' = 0.03$ m s^{-2}. The barotropic mode is even weaker. For a zonally averaged annual wind stress curl of 2×10^{-8} Nm^{-3} over 40° longitude at 24°N, and for water depth $H = 4000$ m, the barotropic SSH annual amplitude, h_{bt}, can be estimated from the time-varying Sverdrup relationship: $\beta\frac{\partial h_{bt}}{\partial x} = \frac{f\nabla\times\vec{\tau}}{\rho_0 g H}$ [*Vivier et al.*, 1999]. The annual amplitude, h_{bt}, increases from zero at the eastern end of the domain to 0.6 cm at the western end. Recall that both the trapped waves and the basin-scale non-propagating signal are larger than 2 cm. We conclude that the annual SSH oscillation northeast of the Hawaiian Islands is not likely to be simply a direct response to the local wind stress curl forcing.

[14] We hypothesize that the trapped annual waves are baroclinic Rossby waves. To support this point of view, $1/k_r$ and $1/k_i$ in equation (1), as estimated by fitting the satellite observations, are compared with those of free Rossby waves in a $1^1/_2$ -layer reduced gravity model, which consists of an active upper layer and a motionless lower layer. The Rossby waves are governed by the conservation law of the upper layer potential vorticity: $\frac{D}{Dt}\Pi = 0$, in which $\Pi \approx f + \xi - f_0\frac{\eta}{H_0}$ [*Pedlosky*, 1987], where f is the Coriolis parameter, ξ the relative vorticity, f_0 the value of f at 24°N, H_0 the mean thickness of the upper layer, and η the perturbation of the upper layer thickness. In the xoy coordinate shown in Figure 2a, the Coriolis parameter $f \approx f_0 + \beta\, x\cos(\alpha) + \beta\, y \sin(\alpha)$, where β the latitudinal derivative of f. Linearizing $\frac{D}{Dt}\Pi = 0$ yields the following Rossby wave equation:

$$\frac{\partial}{\partial t}\left(\xi - f_0\frac{\eta}{H_0}\right) + u\beta\cos(\alpha) + v\beta\sin(\alpha) = 0, \qquad (3)$$

where u and v are the velocities in the x and y directions. Since the lower layer is motionless, the hydrostatic approximation results in $\eta = \frac{g}{g'}h$, where h is the SSH. In addition, the geostrophic approximation is applied: $u = -\frac{g}{f_0}\frac{\partial h}{\partial y}$ and $v = \frac{g}{f_0}\frac{\partial h}{\partial x}$, then $\xi = \frac{g}{f_0}\left(\frac{\partial^2 h}{\partial x^2} + \frac{\partial^2 h}{\partial y^2}\right)$. Equation (3) is thus written as

$$\frac{\partial}{\partial t}\left(\frac{\partial^2 h}{\partial x^2} + \frac{\partial^2 h}{\partial y^2} - \frac{h}{R^2}\right) + \beta\sin(\alpha)\frac{\partial h}{\partial x} - \beta\cos(\alpha)\frac{\partial h}{\partial y} = 0, \qquad (4)$$

where $R = \sqrt{g'H_0}/f_0$ is the internal Rossby radius.

[15] In the following we assume that the Rossby wave crests are parallel to the Hawaiian Islands so that $\partial h/\partial y = \partial^2 h/\partial y^2 = 0$; this is indicated by the relatively clear patterns in the annual amplitudes of the SSH (Figure 3a) and in the annual phase of the along-islands geostrophic flow (Figure 3d). As a result, the simplified $1^1/_2$ -layer reduced gravity model for free Rossby waves is

$$\frac{\partial}{\partial t}\left(\frac{\partial^2 h}{\partial x^2} - \frac{h}{R^2}\right) + \beta\sin(\alpha)\frac{\partial h}{\partial x} = 0. \qquad (5)$$

Assume h takes the form $h \sim e^{i(kx-\omega t)}$, where ω is the annual frequency and k is the wavenumber. Equation (5) yields

$$k = -\frac{\beta\sin(\alpha)}{2\omega} \pm \frac{1}{\omega R}\sqrt{\left(\frac{\beta R\sin(\alpha)}{2}\right)^2 - \omega^2}. \qquad (6)$$

When the radicand in equation (6) is less than zero (i.e., k has an imaginary part: $k = k_r + \mathbf{i}\, k_i$), the Rossby waves are trapped to the islands. In Figure 4, $1/k_r$ and $1/k_i$ are plotted as functions of α. Notice that $1/k_r$ is independent of R but $1/k_i$ depends on both R and α. As shown in Figure 4, the $1/k_r$ from fitting the satellite observations is close to the modeled one; the modeled $1/k_i$ (decay scale) is sensitive to R as well as to α. When $\alpha \approx 20°$, which approximates the orientation of the Hawaiian Islands (Figure 2a), R in the range of 50–60 km [*Chelton et al.*, 1998], and β at 24°N, the fitted $1/k_i$ falls within the range of the modeled ones. Therefore, the trapped annual Rossby wave hypothesis appears promising.

[16] Meanwhile, it is worthwhile mentioning that our fairly good comparison merely demonstrated that the trapped annual waves can be approximately described by using the trapped annual Rossby waves. We do not reveal how the annual waves are generated. One possible mechanism is the resonant forcing by a weak wind stress curl, since the trapped annual Rossby waves obey the homogeneous equation (equation (5)). Another possible generating mechanism is through Rossby wave reflection at the islands [*Mysak and Magaard*, 1983]; notice the apparent amplitude minimum near the islands ($x = 0$, Figure 3a). With respect to the basin-scale non-propagating signal, its generation mechanism remains obscure to us.

4. Concluding Remarks

[17] We have described the SSH annual signals northeast of the Hawaiian Islands in terms of trapped annual waves with crests parallel to the islands and a basin-scale non-propagating signal. Although the signals (2–4 cm) account for only about 10% of the variance of the high-passed (two-

year cutoff) altimetry SSH adjacent to the Hawaiian Islands and about 25% in the interior, the coherent structures, especially after expressed as a function of the distance away from the Hawaiian Islands, indicate that the signals are robust. We hypothesized that the trapped annual waves are baroclinic Rossby waves. Using the linearized vorticity equation, we showed that annual Rossby waves are trapped along the Hawaiian Islands if their crests are parallel to the islands.

[18] The trapped annual waves are important dynamically since they generate geostrophic flows. By seasonally modulating the mean flow associated with the subtropical gyre, the trapped annual waves can in turn modulate seasonally the eddy field if eddies are generated through baroclinic instability of the mean flow. The timing between the seasonally varied mean flow and the seasonally modulated eddy field is an important index in identifying the baroclinic instability mechanism. This mechanism has been successfully demonstrated for the North Pacific and South Pacific subtropical countercurrents [*Qiu*, 1999; *Qiu and Chen*, 2004]. Whether the baroclinic instability mechanism applies to the present region will be the focus of our follow-up research.

[19] **Acknowledgments.** The merged T/P and ERS-1/2 altimeter data are provided by the CLS Space Oceanography Division as part of the Environment and Climate EU ENACT project and with support from CNES. Support from NASA through Contracts 1207881 and 1228847 is gratefully acknowledged. Comments made by Ted Durland, Paulo Calil, and the anonymous reviewers helped improve the manuscript significantly.

References

Bingham, F. M., and R. Lukas (1996), Seasonal cycles of temperature, salinity, and dissolved oxygen observed in the Hawaii Ocean time-series, *Deep Sea Res., Part II*, *43*, 199–213.

Chelton, D. B., R. A. deSzoeke, M. G. Schlax, K. El Naggar, and N. Siwertz (1998), Geographical variability of the first baroclinic Rossby radius of deformation, *J. Phys. Oceanogr.*, *28*, 433–460.

Chiswell, S. M. (1996), Intra-annual oscillations at station ALOHA, north of Oahu, Hawaii, *Deep Sea Res., Part II*, *43*, 305–319.

Jacobs, G. A., W. J. Emery, and G. H. Born (1993), Rossby waves in the Pacific Ocean extracted from Geosat altimeter data, *J. Phys. Oceanogr.*, *23*, 1155–1175.

Kessler, W. S. (1990), Observations of long Rossby waves in the northern tropical Pacific, *J. Geophys. Res.*, *95*(C4), 5183–5217.

Mitchum, G. T. (1996), On using satellite altimetric heights to provide a spatial context for the Hawaii Ocean Time-series measurements, *Deep Sea Res., Part II*, *43*, 257–280.

Mysak, L. A., and L. Magaard (1983), Rossby wave driven Eulerian mean flows along non-zonal barriers, with application to the Hawaiian Ridge, *J. Phys. Oceanogr.*, *13*, 1716–1725.

Pedlosky, J. (1987), *Geophysical Fluid Dynamics*, 2nd ed., 710 pp., Springer, New York.

Polito, P. S., O. T. Sato, and W. T. Liu (2000), Characterization and validation of the heat storage variability from TOPEX/Poseidon at four oceanographic sites, *J. Geophys. Res.*, *105*(C7), 16,911–16,922.

Qiu, B. (1999), Seasonal eddy field modulation of the North Pacific subtropical countercurrent: TOPEX/Poseidon observations and theory, *J. Phys. Oceanogr.*, *29*, 2471–2486.

Qiu, B., and S. Chen (2004), Seasonal modulations in the eddy field of the South Pacific Ocean, *J. Phys. Oceanogr.*, *34*, 1515–1527.

Stammer, D. (1997), Steric and wind-induced changes in TOPEX/Poseidon large-scale sea surface topography observations, *J. Geophys. Res.*, *102*(C9), 20,987–21,009.

Van Woert, M. L., and J. M. Price (1993), Geosat and advanced very high resolution radiometer observations of oceanic planetary waves adjacent to the Hawaiian Islands, *J. Geophys. Res.*, *98*(C8), 14,619–14,631.

Vivier, F., K. A. Kelly, and L. Thompson (1999), Contributions of wind forcing, waves, and surface heating to sea surface height observations in the Pacific Ocean, *J. Geophys. Res.*, *104*(C9), 20,767–20,788.

S. Chen and B. Qiu, Department of Oceanography, University of Hawaii at Manoa, 1000 Pope Road, Honolulu, HI 96822, USA. (schen@soest.hawaii.edu)